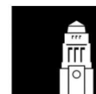

UNIVERSITY OF LEEDS

This is a repository copy of *pH-induced molecular shedding drives the formation of amyloid fibril-derived oligomers*.

White Rose Research Online URL for this paper:
http://eprints.whiterose.ac.uk/91924/

Version: Accepted Version

Article:

Tipping, KW, Karamanos, TK orcid.org/0000-0003-2297-540X, Jakhria, T et al. (6 more authors) (2015) pH-induced molecular shedding drives the formation of amyloid fibril-derived oligomers. Proceedings of the National Academy of Sciences, 112 (18). pp. 5691-5696. ISSN 0027-8424

https://doi.org/10.1073/pnas.1423174112

Reuse
Items deposited in White Rose Research Online are protected by copyright, with all rights reserved unless indicated otherwise. They may be downloaded and/or printed for private study, or other acts as permitted by national copyright laws. The publisher or other rights holders may allow further reproduction and re-use of the full text version. This is indicated by the licence information on the White Rose Research Online record for the item.

Takedown
If you consider content in White Rose Research Online to be in breach of UK law, please notify us by emailing eprints@whiterose.ac.uk including the URL of the record and the reason for the withdrawal request.

eprints@whiterose.ac.uk
https://eprints.whiterose.ac.uk/

pH-induced molecular shedding drives the formation of amyloid fibril-derived oligomers

Kevin W. Tipping, Theodoros K. Karamanos, Toral Jakhria, Matthew G. Iadanza, Sophia C. Goodchild, Roman Tuma, Neil A. Ranson, Eric W. Hewitt and Sheena E. Radford

Astbury Centre for Structural Molecular Biology and School of Molecular and Cellular Biology, University of Leeds, Leeds, LS2 9JT, United Kingdom

Corresponding author: Sheena E. Radford; s.e.radford@leeds.ac.uk; 0113 343 3170

Astbury Centre for Structural Molecular Biology and School of Molecular and Cellular Biology, University of Leeds, Leeds, LS2 9JT, United Kingdom

Other authors: Kevin W. Tipping; bs07kwt@leeds.ac.uk, Theodoros K. Karamanos; t.karamanos@leeds.ac.uk, Toral Jakhria; bstj@leeds.ac.uk, Matthew G. Iadanza; m.iadanza@leeds.ac.uk, Sophia C. Goodchild; s.c.goodchild@leeds.ac.uk, Roman Tuma; r.tuma@leeds.ac.uk, Neil A. Ranson; n.a.ranson@leeds.ac.uk and Eric W. Hewitt; e.w.hewitt@leeds.ac.uk.

Keywords: amyloid, fibrils, membrane disruption, oligomer, disassembly, pH

Abstract

Amyloid disorders cause debilitating illnesses through the formation of toxic protein aggregates. The mechanisms of amyloid toxicity and the nature of species responsible for mediating cellular dysfunction remain unclear. Here, using β_2-microglobulin (β_2m) as a model system, we show that the disruption of membranes by amyloid fibrils is caused by the molecular shedding of membrane-active oligomers in a process that is dependent on pH. Using thioflavin T (ThT) fluorescence, NMR, EM and fluorescence correlation spectroscopy (FCS), we show that fibril disassembly at pH 6.4 results in the formation of non-native spherical oligomers that disrupt synthetic membranes. By contrast, fibril dissociation at pH 7.4 results in the formation of non-toxic, native monomers. Chemical cross-linking or interaction with hsp70 increases the kinetic stability of fibrils and decreases their capacity to cause membrane disruption and cellular dysfunction. The results demonstrate how pH can modulate the deleterious effects of pre-formed amyloid aggregates and suggest why endocytic trafficking through acidic compartments may be a key factor in amyloid disease.

Significance

Oligomers formed *en route* to amyloid fibrils are thought to be the perpetrators of toxicity in many amyloid disorders. How amyloid fibrils contribute to disease, however, is less clear. Here, using β_2-micoglobulin (β_2m) as a model system, we show that the stability of amyloid fibrils is highly pH-dependent, with mild acidification enhancing the formation of fibril-derived non-native oligomers that disrupt membranes and alter cellular function. Enhancing fibril stability by incubation with the molecular chaperone, hsp70, or by cross-linking, protects against fibril-induced membrane disruption and cellular dysfunction. The results highlight the importance of pH in determining fibril stability and suggest that uptake of fibrils into acidic cellular compartments may contribute to amyloid disease by pH-induced molecular shedding of toxic species.

\body

Introduction

Amyloid assembly involves the formation of an ensemble of aggregate species that lead to the onset of pathological cascades and disease (1). The formation of amyloid is initiated by self-association of partially unfolded or intrinsically disordered precursors which stimulates the production of an array of oligomeric assembly intermediates. These species, which precede the formation of mature amyloid fibrils, are commonly described as the agents of toxicity in amyloid disease (1). The ephemeral nature of oligomeric species, combined with their heterogeneity and co-population with other species, provides immense challenges for characterising amyloid assembly intermediates in structural detail and determining their role(s) in fibril assembly (1). It also highlights the difficulty in identifying which species amongst the aggregate ensemble contributes to cellular dysfunction and the onset of amyloid disease.

Although oligomers formed from many different proteins have been shown to be toxic (2), the role that fibrils play in amyloid disease is not well understood. Mounting evidence suggests that fibrils can be toxic (3–5), or may contribute to disease by acting as reservoirs of toxic oligomers (6). Fibrils may also contribute to disease by catalysing the formation of oligomers on their surface via secondary nucleation processes (7), or by disrupting protein homeostasis by consuming the capacity of the proteostatic network through the sequestration of molecular chaperones (8). Reduced fibril length can also contribute to disease by increasing the uptake of fibrils into intracellular compartments (9–11), or by enhancing transmission of aggregation between cells in prion-like processes (12). In addition, fibrils have been shown to interact with lipid bilayers, causing membrane deformations via interactions with fibril ends (10, 13, 14), or promoting the release of toxic oligomers by membrane-induced fibril disassembly (15). Together these data support a role of amyloid fibrils as direct or indirect agents of amyloid disease.

Since amyloid formation is under kinetic control, minor changes in the population of an amyloid precursor can lead to dramatic changes in the rate of fibril formation and in the repertoire of

oligomeric species formed (16, 17). Conversely, the kinetic stability of amyloid fibrils can be enhanced by alterations in the protein sequence (18), or by adding small molecules (19, 20) or molecular chaperones (21). Such enhancements in fibril stability can protect against toxicity, presumably by supressing the formation of oligomers. In addition, fibrils may encounter environments *in vivo* that are distinct from those which promote their formation; yet how localised cellular environments affect the dynamic equilibrium of amyloid fibrils remains unclear.

Here, using amyloid fibrils formed *in vitro* from β_2-microglobulin (β_2m) as a model system, we explore the effect of altering pH on fibril stability and in determining the nature of the soluble products that result from fibril disassembly. Using biochemical, biophysical and cellular assays, we show that β_2m fibril disassembly is highly sensitive to changes in pH, with a reduction in pH from 7.4 to 6.4 (similar to the difference in pHs encountered early during endocytic trafficking) resulting in dramatically different outcomes of disassembly. The results reveal how subtle changes in pH can alter the delicate kinetic balance of intermediates in fibrillation reactions and suggest that increasing fibril stability, and/or decreasing fibril uptake into acidic cellular compartments, may be a viable strategy to alleviate the progression of amyloid disease.

Results

pH dependent fibril dynamics

To investigate how pH alters the stability and dynamic behaviour of amyloid fibrils, β_2m monomers were assembled into amyloid fibrils by incubation at acidic pH (Methods). These fibrils have been analysed structurally in detail and have been shown to possess the canonical parallel in-register β-sheet amyloid structure formed by many proteins and peptides, including β_2m fibrils isolated *ex vivo* (22, 23). In addition, β_2m fibrils formed under acidic conditions are structurally similar to those formed *in vitro* at near-neutral pH from the N-terminally truncated β_2m variant, ΔN6 (22). They also display similar effects (internalisation into the endo-lysosomal pathway and the inhibition of cellular reduction of MTT) when incubated with cell lines and with primary cells relevant to the pathology of β_2m dialysis-related amyloidosis (DRA) (monocytes, chondrocytes and osteoblasts) (10, 11, 24, 25). Moreover, fibrils formed from ΔN6, but seeded with wild-type β_2m fibrils formed at low pH, have

been shown to inhibit osteoclast formation from primary human monocytes, hence rationalizing the osteoarticular pathology associated with DRA (24).

The kinetic stability of the β_2m fibrils was measured by diluting fibrils formed at acidic pH into buffer at pH 7.4 or 6.4 (at an identical ionic strength of 164 mM (Methods)). pH values of 7.4 and 6.4 were chosen to mimic the environments encountered by fibrils in the extracellular milieu and in early endosomes, respectively. In previous experiments we have shown that β_2m fibrils are taken up into endosomes and lysosomes in a length-dependent manner, wherein they persist as protease-resistant material that retains a cross-β structure and results in the perturbation of lysosome function (11, 24, 25). pH-induced changes in fibril yield and conformation were monitored by ThT fluorescence and SDS PAGE (Methods). Dilution into each buffer resulted in an initial increase in ThT fluorescence, presumably due to alterations in ThT binding sites in the fibril-bound state (26), followed by a slow phase in which the fluorescence intensity decreases (Fig. 1A,B). Fitting to a double exponential revealed that the rate constants for the enhancement and decay of fluorescence are similar at both pH values (Fig. S1A-D). Most strikingly, however, the amplitude of the second phase of the reaction is larger at pH 7.4 than 6.4 (corresponding to 94 % and 55 % at each pH, respectively). At both pH values, SDS-PAGE analysis of soluble material revealed that the rate of loss of ThT fluorescence mirrors the rate at which soluble material is formed (Fig. 1A,B). Analysis of the fibril length distributions using AFM 30 and 60 min after sample dilution at pH 7.4 or 6.4, respectively, (at which times *ca.* 25 % soluble material is formed (Fig. 1A,B)), showed a reduction in fibril length upon incubation at both pH values (Fig. S1E,F). Similar effects were not observed upon diluting fibrils into growth buffer at pH 2.0 (Fig. S1G). Moreover, mutation of each of the three His residues known to reside within the core of β_2m fibrils (22) significantly decreased the pH dependency of the loss of ThT fluorescence (Fig. S2), suggesting the protonation state of these His residues plays a role in determining the extent of pH-dependent fibril disassembly leading to the formation of soluble material.

The mechanism of fibril depolymerisation is pH-dependent

To determine the nature of soluble species released during fibril disassembly, fibril depolymerisation was monitored at pH 6.4 and 7.4 using ^{1}H-^{15}N NMR and the appearance of resonances was monitored in real time (Figs. 2A,B and S3). Most resonances that were detected have a chemical shift identical to those of the native protein, enabling the rate of production of native species to be determined at each pH (Fig. 2C,D). The results revealed that at each pH native amide resonances increase in intensity at a similar rate across the sequence of β_2m (Fig. 2C,D). However the average rate of appearance of native resonances is dependent on the pH. The average per-residue time constant (τ) for the appearance of native β_2m resonances at pH 7.4 (105 ± 7 min) mirrors τ for the decay in ThT fluorescence (95 ± 5 min) (Fig. 2C), indicating that fibril disassembly leads to the formation of native β_2m monomers. At pH 6.4, by contrast, although the decrease in ThT fluorescence (99 ± 6 min) occurs at a similar rate to the appearance of soluble material (Fig. 1B), the appearance of native β_2m resonances measured using NMR is delayed significantly (171 ± 10 min, Fig. 2D). This suggests that fibril disassembly at pH 6.4 results in the formation of NMR-invisible species that precede the development of native and unfolded monomers. Indeed, weak resonances with chemical shifts distinct from those of the native monomer are detected early during fibril depolymerisation at pH 6.4, but not at pH 7.4 (Fig. S4), suggesting that the 'NMR invisible' species are non-native, but not unfolded. The absence of a detectable lag in the appearance of the native resonances at pH 6.4 suggests that the NMR invisible non-native species could be off-pathway. Alternatively, an on-pathway model in which the exchange rate for oligomer formation does not exceed significantly the rate of monomer formation would also fit the data. More experimental data will be needed to resolve this issue. Irrespective of the kinetic model for their formation, however, the results show that reducing the pH by a single unit alters the kinetics, and/or kinetic mechanism, of fibril disassembly such that non-native species accumulate only at the lower pH.

Oligomeric species accumulate during fibril disassembly at pH 6.4

To characterise and compare the soluble species that form during fibril disassembly in more detail

fluorescence correlation spectroscopy (FCS) was used. FCS exploits fluctuations in fluorescent signals as molecules diffuse through a confocal volume of known size (see SI for more detail). Given its ability to detect species that differ in size over several orders of magnitude, in complex ensembles and without purification, FCS is an ideal technique to identify and track the ensemble of species that form during amyloid assembly/disassembly over time.

Fibril depolymerisation was measured using FCS by labelling the β_2m variant R3C with maleimide-Alexa488 (R3C488) (Methods). Residue 3 was chosen as the site to incorporate a fluorescent label as the N-terminal six residues of β_2m do not form part of the fibril core (27). R3C488 was incorporated into fibrils by seeded elongation in the presence of a 1000-fold molar excess of wild-type β_2m monomers. Fibril depolymerisation was then initiated by diluting these samples into pH 7.4 or 6.4 buffer. Autocorrelation curves (ACs) were acquired immediately and over the course of depolymerisation (Methods and SI text) (Figs. S5 and S6). The curves were fitted using a maximum entropy method (MEM) (28) to extract the apparent hydrodynamic radius (R_H) of soluble species released from fibrils during depolymerisation (see SI text for details).

The FCS analysis revealed that soluble species released over the course of fibril depolymerisation at pH 7.4 are dominated by a low molecular weight species with an apparent R_H of 1.9 nm (Fig. 3A, left panels), equivalent to the apparent R_H determined for native β_2m monomers (Fig. S7). By contrast, at pH 6.4 a second species with an apparent R_H of 20 nm is highly populated and persists up to 135 min after the initiation of disassembly (Fig. 3A, right panels). Fitting the ACs to simpler one or two component functions confirmed that this larger species is only populated significantly during fibril disassembly at pH 6.4 (Fig. S8, Tables S1 and S2). Analysis of samples 30 min (pH 7.4) or 60 min (pH 6.4) after initiating depolymerisation using negative stain TEM (Fig. 3B,C) revealed the presence of spherical oligomers at pH 6.4, but not at pH 7.4. These species range in diameter from 30-60 nm, measured using cryo-EM (Fig. 3D-E, Fig. S9). Previous studies have shown that oligomers of this size do not accumulate during fibril formation of ΔN6 at pH 6.2 or from wild-type β_2m at pH 2.0, and thus their accumulation is a unique consequence of fibril disassembly at pH 6.4

(17, 29). Further structural characterisation revealed that these species are not recognised by the antibody WO1 (which recognises the cross-β fold of amyloid (30)) (Fig. 4A and SI Methods) and give rise to a far UV CD spectrum consistent with significant non-native (more highly unfolded) structure (Fig 4C). By contrast, CD analysis of the soluble species released at pH 7.4 is consistent with the formation of predominantly native species (Fig. 4B). The oligomers formed at pH 6.4 also expose greater hydrophobic surface area than those at pH 7.4, measured by the fluorescence of the hydrophobic dye, 8-anilinonaphthalene-1-sulphonate (ANS) (Fig. 4D,E). Together, the results indicate that pH alters the energy landscape of fibril depolymerisation such that non-native, spherical oligomers only become highly, and persistently, populated at pH 6.4.

Fibril-released oligomers cause membrane disruption

The ability of oligomers produced during fibril disassembly at pH 6.4 to disrupt membranes was next examined by an *in vitro* dye release assay using large unilamellar vesicles (LUVs) containing 12 mol% bismonoacylphosphate (BMP). BMP is enriched in endosomal/lysosomal membranes and has been shown previously to sensitise LUVs to disruption by β_2m amyloid fibrils (13). The disruption of BMP-containing membranes by β_2m fibrils is also pH dependent, with a large increase in the extent of membrane disruption observed when the pH is decreased from 7.4 to 6.4 (13). To determine the extent of membrane disruption caused by soluble species released during fibril depolymerisation, β_2m fibrils were allowed to depolymerise for 60 min at pH 6.4. Filtration was then used to separate soluble species from fibrillar material, so that the effect of each fraction on membrane integrity could be assessed individually. These experiments showed that the soluble material released from fibrils accounts for *ca.* 70 % of the membrane disruption activity of the total (fibril + soluble) sample (Fig. 5A). Determining the dye release efficiency per µM protein showed that the soluble material is *ca.* 5-times more membrane active than the same monomer-equivalent concentration of β_2m fibrils (Fig. 5B). As native β_2m monomers cause minimal dye release (Fig. 5A,B), non-native oligomers that accumulate during fibril disassembly at pH 6.4 must be responsible for the majority of fibril-mediated membrane disruption.

Restricting molecular shedding decreases membrane damage and fibril-mediated cellular dysfunction

To determine whether fibril-induced membrane damage can be inhibited by enhancing the kinetic stability of β_2m amyloid fibrils, the molecular chaperone hsp70 was added. Previous studies have shown that the association of hsp70 (or its constitutively expressed homologue, hsc70) with amyloid aggregates protects against amyloid toxicity (31–33). Recombinant hsp70-1A (32) was incubated with β_2m amyloid fibrils at pH 6.4 in a 1:0.25 or 1:3 molar ratio (monomer equivalent β_2m:chaperone) and the effect of the chaperone on fibril stability was measured using ThT fluorescence. These experiments showed that hsp70 enhances the kinetic stability of β_2m fibrils such that no depolymerisation is observed up to 3 h after dilution to pH 6.4 (Fig. 5C). To determine whether the addition of hsp70 also affects the ability of β_2m fibrils to mediate membrane disruption, LUVs containing 12 mol% BMP were incubated with fibrils in the presence of hsp70 (Fig. 5D). These experiments showed that membrane disruption is decreased significantly in the presence of both 0.25 and 3 molar equivalents of hsp70, in comparison with controls lacking hsp70. The residual membrane disruption activity is presumably attributed to the activity of the fibrils themselves (Fig. 5A,B (14)). Chemically cross-linking fibrils to enhance their stability also resulted in a significant decrease in membrane disruption (Fig. S10A-C).

Finally, to determine whether hsp70 is able to protect cells against fibril-induced cellular dysfunction, SH-SY5Y cells were incubated with either 0.3 µM or 3 µM hsp70 for 6 h prior to adding 1.2 µM (monomer equivalent concentration) of β_2m fibrils. Previous studies have shown that β_2m fibrils inhibit MTT reduction without causing cell death (11). Instead, fibrils disrupt lysosomal function as evidenced by the inhibition of the degradation of endocytosed ovalbumin (11). Here, hsp70 was shown to rescue cells from fibril-mediated inhibition of MTT reduction when pre-incubated with 3 µM hsp70 prior to the addition of β_2m fibrils (Fig. 5E). Similarly, the reduction in the capacity of cells to degrade ovalbumin taken up by endocytosis in the presence of β_2m fibrils (11) was restored in hsp70 treated cells (Fig. 5F). Thus, an excess of hsp70 is able to protect against the deleterious effects of β_2m fibrils measured by these two assays. Decreasing the extent of fibril depolymerisation

by chemical cross-linking also partially rescued the inhibition of MTT reduction by fibrils (Fig. S10D). Together, these results suggest that the pH-dependent shedding of oligomers from fibrils contributes to β_2m fibril-mediated membrane disruption *in vitro* and to cellular dysfunction, firmly ascribing the formation of these previously uncharacterised fibril-derived oligomers as facilitators of amyloid-induced cellular degeneration.

Discussion

Although amyloid fibrils have been shown previously to exhibit dynamic behaviour in solution (6, 34), the importance of such dynamic excursions in the context of biological activity has remained unclear. Here, by studying amyloid fibril dynamics in solution conditions distinct from those which promote aggregation and, most importantly, which mimic the cellular environment encountered early during endocytosis, we show how subtle differences in pH can dramatically influence the repertoire of species that form over the course of fibril disassembly *in vitro*. The importance of histidine residues in controlling the fate of β_2m fibril disassembly suggests that other amyloid assemblies may also display pH-dependent depolymerisation pathways, especially for fibrils that are formed extracellularly and trafficked via the endocytic pathway. As shown here using β_2m fibrils formed *in vitro* as a model, a change in the pH by just one unit (pH 7.4 to 6.4) dramatically enhances the potential of fibrils to act as vehicles of cellular dysfunction by enhancing the accumulation of non-native oligomers able to disrupt membranes *in vitro* and to contribute to cellular dysfunction.

The endo-lysosomal pathway is emerging as a common route by which extracellular and intracellular amyloid aggregates can elicit mechanisms of toxicity (35, 36). For β_2m fibrils, cellular dysfunction is associated with internalisation via endocytosis, with fibril uptake being enhanced for fibrils of short average length (<400 nm), such as those produced early during fibril formation or via fibril fragmentation (10). Long-term residence of protease-resistant fibrils within lysosomes leads to perturbation of the ability of these organelles to degrade endocytosed proteins (11, 25). Moreover, recent investigations have shown that synthetic membranes containing BMP, a lipid enriched in endosomes and lysosomes (37), have enhanced susceptibility to β_2m fibril-mediated membrane disruption compared with synthetic membranes lacking BMP (13). Together, decreased kinetic

stability of fibrils under mildly acidic conditions, combined with the specific lipid composition of endosomes/lysosomes, creates a cellular environment that is uniquely susceptible to β_2m amyloid fibril-mediated cellular damage.

The results presented here also demonstrate that increasing the stability of amyloid fibrils by chemical cross-linking or the addition of hsp70 leads to decreased membrane disruption and a reduction in lysosome dysfunction. Hsp70 has been shown to inhibit aggregation and toxicity of a variety of amyloidogenic systems via distinct mechanisms (31–33). Here we show that hsp70 is able to protect cells against the deleterious effects of β_2m fibril-mediated cell dysfunction to a greater extent than chemical cross-linking. This suggests that hsp70 inhibits fibril-mediated cellular dysfunction by preventing molecular shedding, and potentially through additional mechanisms. Nevertheless, the results suggest that the pH-induced formation of fibril-derived oligomers is a significant source of β_2m fibril-mediated cellular dysfunction. pH-induced molecular shedding may also contribute to fibril-mediated toxicity of other amyloid aggregates that undergo endocytic trafficking. For example, the stabilisation of fibrils by small molecules has been shown to reduce Aβ toxicity by accelerating assembly towards β-rich fibrils (19). Other studies have shown that small molecules can alleviate Aβ fibril-mediated toxicity (20), presumably by stabilising fibrils and preventing the shedding of toxic species. Further studies using other amyloid systems are now needed to determine in more detail the role of the endo-lysosomal pathway in modulating fibril/aggregate stability and hence in contributing to the protection or exacerbation of disease.

By contrast with protein folding reactions which, in most cases, result in the formation of a unique structural entity (the native state), amyloid formation is a complex kinetic process that can give rise to fibrils and aggregates with distinct structural, kinetic and/or thermodynamic properties (9, 38). For example, structurally distinct fibrils of α-synuclein, and those of Aβ, display different biological activities (9, 39, 40). Depending on their structure, some fibril strains will be less kinetically stable than others and, thereby, could potentially be more dangerous biologically than their similar, but more stable counterparts. In addition, as shown here for β_2m, subtle changes in solution conditions can change the repertoire of oligomers originating from a single fibril strain by altering the energy

landscape of fibril disassembly. Rather than being the innocuous end products of assembly, fibrils may thus be a dangerous source of toxic oligomers uniquely formed by molecular shedding in a mechanism that is dependent on the pH. A better understanding of the link between fibril dynamics, pH and toxicity, such as presented here for β_2m fibrils, may provide new avenues for the development of therapeutic strategies against amyloid disease.

Materials and Methods

More details can be found in SI text.

Protein expression, purification and labelling

Wild-type β_2m, ^{15}N-labelled β_2m and β_2m R3C were expressed and purified as previously described (10, 17, 27). The R3C variant was covalently labelled with maleimide-Alexa488 (Invitrogen) according to manufacturer's instructions. Labelled monomer was stored at -80°C in 25 mM sodium phosphate buffer, pH 7.2. The human hsp70-1A gene was kindly provided by Chris Dobson (University of Cambridge) and was expressed and purified as described (32).

Fibril formation and kinetic stability assay

Fibril samples were prepared by dissolving lyophilised β_2m monomers in 10 mM sodium phosphate buffer, pH 2.0 containing 50 mM NaCl. The sample was filtered (0.22 µM Millipore syringe filter) and the protein concentration adjusted to 120 µM (monomer equivalent concentration). Fibril formation was seeded using 0.1 % (*w/w*) of preformed β_2m fibrils as previously described (10). Samples were then incubated quiescently at room temperature for 48 h. This resulted in fibrils of average length ~1.2 µm measured using AFM, consistent with previous results (10, 13). These fibrils were used for all subsequent experiments.

To monitor the stability of β_2m fibrils upon changes in pH, β_2m fibrils (120 µM monomer equivalent concentration) were diluted 4-fold into 50 mM sodium phosphate buffer, pH 7.4 containing 35 mM NaCl, or 50 mM sodium phosphate buffer, pH 6.4 containing 85 mM NaCl (ionic strength 164 mM), previously equilibrated at 25°C and supplemented with 10 µM ThT. ThT fluorescence was

measured using a BMG Labtech Optima plate reader with excitation and emission band passes of 440 ± 5 nm and 480 ± 5 nm for up to 360 min. ThT fluorescence curves were fitted to a double exponential function. Errors represent the standard deviation of a minimum of 20 replicates. Soluble material was also measured as a function of time by SDS PAGE following filtration to separate fibrils from soluble material (see SI Methods).

NMR

For NMR experiments, depolymerisation of ^{15}N-labelled β_2m fibrils was initiated by dilution to a final (monomer equivalent) concentration of 150 μM into the pH 7.4 or pH 6.4 buffers described above. Each buffer was supplemented with 10% (*v/v*) D_2O and 50 μM ThT (the latter was included to enable direct comparison with the rates of fibril depolymerisation, measured at the same time using the same stock of fibrils, by ThT fluorescence). The appearance of NMR-observable species was then monitored over time by acquiring SOFAST ^{1}H-^{15}N HSQC spectra (41) at 25°C using a Varian Inova spectrometer (Agilent) at a ^{1}H frequency of 750MHz, equipped with a cryogenic probe. The dead time of the experiment was 3-7 min and the acquisition time of individual spectra varied between 5 – 10 min (4 and 8 scans per incremental delay, respectively). At least 20 sequential ^{1}H-^{15}N HSQC spectra were acquired with a final acquisition (of 100% native monomer) performed 24 h after the initial dilution. The experiment was repeated several times, increasing the spectral acquisition time to optimise the signal-to-noise ratio, while maintaining time resolution. The average of two such experiments is shown in Figure 2. The error bars represent the propagated error of the fits to single exponentials for each residue over the two experiments.

FCS

Details of the instrument set-up, data collection and analysis can be found in SI text.

Hsp70 binding and cell assays

The kinetic stability of β_2m amyloid fibrils in the presence of hsp70 was monitored by diluting fibrils formed at pH 2.0 to 12 μM (monomer equivalent concentration) in pH 6.4 buffer to which 0, 0.25 or 3 molar equivalents of recombinant hsp70-1A or 3 molar equivalents of BSA were added.

Depolymerisation was then monitored at 25°C by ThT fluorescence as outlined above. Data shown are the average from a minimum of three independent replicates.

MTT and lysosome proteolysis assays were performed on SH-SY5Y cells as previously described (11). Cells were cultured in the presence of 0, 0.3 or 3.0 μM hsp70 for 6 h prior to the addition of 1.2 μM (monomer equivalent concentration) of fibrils that had been fragmented for 48 h as previously described (10). Native β_2m monomer, buffer-only, hsp70-only, or 0.1% (*w/v*) sodium azide were added as controls. For the MTT assay, cells were incubated for a further 24 h prior to the addition of 20 µl 5mg.ml^{-1} MTT. After further incubation for 60 min the media was removed and the resulting formazan crystals were solubilised in 100% dimethyl sulfoxide. Reduction of MTT was quantified by measuring the absorbance at 570 nm and subtracting background light scattering at 650 nm. The error bars represent the standard deviation from three independent experiments, each containing five replicates. Details of the lysosome proteolysis assay can be found in SI Methods.

Acknowledgements

We thank Jennifer Clark, Alex Borodavka and members of the Radford group for helpful discussions and Aneika Leney for preparing the β_2m mutants. We also thank Sudipta Maiti for providing the MEM analysis scripts. We acknowledge financial support from the Wellcome Trust (093794/Z/10/Z (K.W.T.), 089311/Z/09/Z (T.K.K.), 092896 (S.C.G, E.W.H. and S.E.R.) 090932/Z/09/Z and 094232/Z/10/Z (EM, CD and NMR equipment), BBSRC (BB/526502/1 (T.J.)), and the ERC ((FP7/2007-2013) / ERC grant agreement n°32240 (T.K.K., M.G.I., N.A.R., E.W.H. and S.E.R.)).

References

1. Knowles TPJ, Vendruscolo M, Dobson CM (2014) The amyloid state and its association with protein misfolding diseases. *Nat Rev Mol Cell Biol* 15:384–396.

2. Kayed R, et al. (2003) Common structure of soluble amyloid oligomers implies common mechanism of pathogenesis. *Science* 300:486–489.

3. Pieri L, Madiona K, Bousset L, Melki R (2012) Fibrillar α-synuclein and huntingtin exon 1 assemblies are toxic to the cells. *Biophys J* 102:2894–2905.

4. Mossuto MF, et al. (2010) The non-core regions of human lysozyme amyloid fibrils influence cytotoxicity. *J Mol Biol* 402:783–796.

5. Nekooki-Machida Y, et al. (2009) Distinct conformations of in vitro and in vivo amyloids of huntingtin-exon1 show different cytotoxicity. *Proc Natl Acad Sci USA* 106:9679–9684.

6. Cremades N, et al. (2012) Direct observation of the interconversion of normal and toxic forms of α-synuclein. *Cell* 149:1048–1059.

7. Cohen SI, et al. (2013) Proliferation of amyloid-β_{42} aggregates occurs through a secondary nucleation mechanism. *Proc Natl Acad Sci USA* 110:9758–9763.

8. Olzscha H, et al. (2011) Amyloid-like aggregates sequester numerous metastable proteins with essential cellular functions. *Cell* 144:67–78.

9. Bousset L, et al. (2013) Structural and functional characterization of two alpha-synuclein strains. *Nat Commun* 4:2575.

10. Xue W-F, et al. (2009) Fibril fragmentation enhances amyloid cytotoxicity. *J Biol Chem* 284:34272–34282.

11. Jakhria T, et al. (2014) β_2-microglobulin amyloid fibrils are nanoparticles that disrupt lysosomal membrane protein trafficking and inhibit protein degradation by lysosomes. *J Biol Chem* 289:35781–35794.

12. Aulić S, et al. (2014) Defined α-synuclein prion-like molecular assemblies spreading in cell culture. *BMC Neurosci*:doi:10.1186/1471–2202–15–69.

13. Goodchild SC, et al. (2014) β_2-microglobulin amyloid fibril-induced membrane disruption is enhanced by endosomal lipids and acidic pH. *PLoS One* 9:e 104492.

14. Milanesi L, et al. (2012) Direct three-dimensional visualization of membrane disruption by amyloid fibrils. *Proc Natl Acad Sci UA* 109:20455–20460.

15. Martins IC, et al. (2008) Lipids revert inert Aβ amyloid fibrils to neurotoxic protofibrils that affect learning in mice. *EMBO J* 27:224–233.

16. Buell AK, et al. (2011) Population of nonnative states of lysozyme variants drives amyloid fibril formation. *J Am Chem Soc* 133:7737–7743.

17. Karamanos TK, Kalverda AP, Thompson GS, Radford SE (2014) Visualization of transient protein-protein interactions that promote or inhibit amyloid assembly. *Mol Cell* 55:214–226.

18. Ramirez-Alvarado M, Merkel JS, Regan L (2000) A systematic exploration of the influence of the protein stability on amyloid fibril formation in vitro. *Proc Natl Acad Sci USA* 97:8979–8984.

19. Bieschke J, et al. (2012) Small-molecule conversion of toxic oligomers to nontoxic β-sheet-rich amyloid fibrils. *Nat Chem Biol* 8:93–101.

20. Jiang L, et al. (2013) Structure-based discovery of fiber-binding compounds that reduce the cytotoxicity of amyloid beta. *Elife* 2:e00857.

21. Narayan P, et al. (2014) Rare individual amyloid-β oligomers act on astrocytes to initiate neuronal damage. *Biochemistry* 52:2442–2453.

22. Su Y, et al. (2014) Secondary structure in the core of amyloid fibrils formed from human β_2m and its truncated variant ΔN6. *J Am Chem Soc* 136:6313–6325.

23. Jahn TR, Tennent GA, Radford SE (2008) A common β-sheet architecture underlies in vitro and in vivo β_2-microglobulin amyloid fibrils. *J Biol Chem* 283:17279–86.

24. Porter MY, Routledge KE, Radford SE, Hewitt EW (2011) Characterization of the response of primary cells relevant to dialysis-related amyloidosis to β_2-microglobulin monomer and fibrils. *PLoS One* 6:e27353.

25. Morten IJ, Gosal WS, Radford SE, Hewitt EW (2007) Investigation into the role of macrophages in the formation and degradation of β_2-microglobulin amyloid fibrils. *J Biol Chem* 282:29691–700.

26. Wolfe LS, et al. (2010) Protein-induced photophysical changes to the amyloid indicator dye thioflavin T. *Proc Natl Acad Sci USA* 107:16863–16868.

27. Ladner CL, et al. (2010) Stacked sets of parallel, in-register beta-strands of β_2-microglobulin in amyloid fibrils revealed by site-directed spin labeling and chemical labeling. *J Biol Chem* 285:17137–17147.

28. Sengupta P, Garai K, Balaji J, Periasamy N, Maiti S (2003) Measuring size distribution in highly heterogeneous systems with fluorescence correlation spectroscopy. *Biophys J* 84:1977–1984.

29. Smith AM, Jahn TR, Ashcroft AE, Radford SE (2006) Direct observation of oligomeric species formed in the early stages of amyloid fibril formation using electrospray ionisation mass spectrometry. *J Mol Biol* 364:9–19.

30. O'Nuallain B, Wetzel R (2002) Conformational Abs recognizing a generic amyloid fibril epitope. *Proc Natl Acad Sci USA* 99:1485–1490.

31. Danzer KM, et al. (2011) Heat-shock protein 70 modulates toxic extracellular α-synuclein oligomers and rescues trans-synaptic toxicity. *FASEB J* 25:326–336.

32. Roodveldt C, et al. (2009) Chaperone proteostasis in Parkinson's disease: stabilization of the Hsp70/α-synuclein complex by Hip. *EMBO J* 28:3758–3770.

33. Wang AM, et al. (2013) Activation of Hsp70 reduces neurotoxicity by promoting polyglutamine protein degradation. *Nat Chem Biol* 9:112–118.

34. Carulla N, et al. (2005) Molecular recycling within amyloid fibrils. *Nature* 436:554–558.

35. Desplats P, et al. (2009) Inclusion formation and neuronal cell death through neuron-to-neuron transmission of α-synuclein. *Proc Natl Acad Sci USA* 106:13010–13015.

36. Treusch S, et al. (2011) Functional links between Aβ toxicity, endocytic trafficking, and Alzheimer's disease risk factors in yeast. *Science* 334(6060):1241–5.

37. Kobayashi T, et al. (2002) Separation and characterization of late endosomal membrane domains. *J Biol Chem* 277:32157–32164.

38. Sarell CJ, et al. (2013) Expanding the repertoire of amyloid polymorphs by co-polymerization of related protein precursors. *J Biol Chem* 288:7327–37.

39. Buell AK, et al. (2014) Solution conditions determine the relative importance of nucleation and growth processes in α-synuclein aggregation. *Proc Natl Acad Sci USA* 111:7671–7676.

40. Petkova AT, et al. (2005) Self-propagating, molecular-level polymorphism in Alzheimer's β-amyloid fibrils. *Science* 307:262–265.

41. Schanda P, Kupce E, Brutscher B (2005) SOFAST-HMQC experiments for recording two-dimensional heteronuclear correlation spectra of proteins within a few seconds. *J Biomol NMR* 33:199–211.

Figure Legends

Figure 1. pH dependence of fibril disassembly. β_2m amyloid fibrils formed at pH 2.0 were diluted into (A) pH 7.4 or (B) pH 6.4 buffer and disassembly monitored by ThT fluorescence (solid lines show a fit to a double exponential). Soluble material released as fibril depolymerisation proceeds was isolated using a filter-trap assay, resolved by SDS-PAGE (inset), and quantified by densitometry of the gel (dashed line).

Figure 2. The formation of native β_2m monomers during fibril depolymerisation monitored by real-time NMR. (A) Select regions of ^{1}H-^{15}N HSQC spectra collected at different times during depolymerisation of ^{15}N-labelled β_2m fibrils at pH 7.4 (purple) or pH 6.4 (green). Residue assignments are shown on the bottom panels. (B) The peak intensity of residue 19K versus time during fibril depolymerisation at pH 7.4 (purple) or pH 6.4 (green). The data are fitted to single exponential functions (solid lines). Coloured bars highlight the time-points at which the spectra shown in (A) were acquired (framed in the same colour). (C) Time constants (τ) of appearance of native resonances during fibril depolymerisation at pH 7.4 or (D) pH 6.4. Black dashed lines indicate the average under each condition. Red dashed lines depict τ of ThT fluorescence decay calculated in Fig. 1A,B.

Figure 3. pH dependent formation of oligomers during fibril disassembly. (A) Apparent R_H distributions of soluble species extracted from autocorrelation curves collected by FCS and analysed by MEM at different times during β_2m fibril disassembly at pH 7.4 or pH 6.4. The apparent R_H values shown are the peak centre of each ensemble. Negative stain TEM image of fibrils 30 min or 60 min after the initiation of fibril depolymerisation at (B) pH 7.4 or (C) pH 6.4 (scale bar = 150 nm). (D) Cryo-EM class averages of oligomers released from fibrils at pH 6.4, 5 min after initiating disassembly. Each box is 60 x 60 nm (see also Fig. S9). (E) Histogram showing size distribution of the particles used to compute the class averages in (D).

Figure 4. Structural analysis of soluble material formed during fibril disassembly. (A) Dot

blots of insoluble and soluble material (filtrate) generated 30 min or 60 min after the initiation of fibril disassembly at pH 7.4 or pH 6.4, respectively. Samples were immunoblotted with anti-fibril (W01 (30)) or anti-β_2m antibodies (SI Methods). Control blots are of β_2m fibrils at pH 2.0. Mean residue ellipticity of the filtrate isolated as stated above at (B) pH 7.4 or (C) pH 6.4 measured using far-UV CD. Spectra of native β_2m (blue) were acquired at the same protein concentration (SI Methods). Difference spectra are shown in dashed lines. ANS fluorescence emission spectra of the filtrate isolated as stated above at (D) pH 7.4 or (E) pH 6.4 and of native β_2m at equivalent concentrations. Curves are normalised to the maximum amplitude of the spectrum of acid unfolded β_2m at pH 2.0 (grey dashed line) acquired at the same protein concentration. In (C-E) native β_2m monomer controls are shown in cyan.

Figure 5. Fibril-derived oligomers cause membrane disruption and cellular dysfunction. (A) Membrane disruption of total protein (fibrils + soluble material) versus soluble material (filtrate) isolated 60 min after the initiation of fibril disassembly at pH 6.4 measured using a carboxyfluorescein dye release assay (SI Methods). The dye release of the equivalent concentration (to total protein sample) of native monomers was also measured (native β_2m). (B) Normalised dye release efficiency per μM of protein (determined using SDS-PAGE densitometry). The fibril concentration was calculated as the amount of non-filtrated material present 60 min after the onset of fibril disassembly. (C) Kinetic stability of β_2m fibrils (12 μM monomer equivalent concentration) at pH 6.4 measured using ThT fluorescence in the presence or absence (black dashed) of 0.25 molar (orange) or 3 molar (green) equivalents of hsp70. A control in the presence of a 3-fold molar excess of bovine serum albumin (BSA) is also shown (grey). (D) Membrane disruption by β_2m fibrils 30 min after the initiation of fibril disassembly as measured by dye release in the presence of 0.25 or 3 molar equivalents of hsp70. (E) The reduction of MTT in the presence of 1.2 μM β_2m amyloid fibrils with or without the addition of 0.25 or 3 molar equivalents of hsp70. MTT reduction is expressed as a percentage in comparison with cells incubated with hsp70 in the absence of fibrils. (F) SH-SY5Y cells were incubated with buffer, 1.2 μM (monomer equivalent concentration) native β_2m monomers or fibril samples after pre-incubation in the presence (light

grey) or absence (dark grey) of a 3-fold molar excess of hsp70. The lysosomal degradation of endocytosed Alexa647-labelled ovalbumin was quantified by flow cytometry (11). * represents a p value of <0.05.

A pH 7.4

depolymerisation time (min)

0 2 5 10 20 40 60 120

β_2m

ThT

soluble β_2m

norm. ThT fluorescence

soluble release

time (min)

B pH 6.4

depolymerisation time (min)

0 10 20 40 60 90 120

β_2m

ThT

soluble β_2m

norm. ThT fluorescence

soluble release

time (min)

A
pH 7.4
15 min
pH 6.4
15 min
45 min
65 min
175 min
^{15}N (ppm)
^{1}H (ppm)
24N
19K
44E
65L
55S
49V
97R
87L
35I
84H
85V
37V
36E
99M

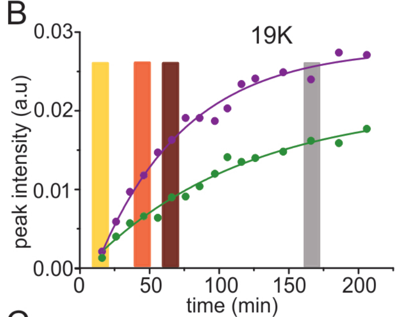
B
19K
peak intensity (a.u)
time (min)

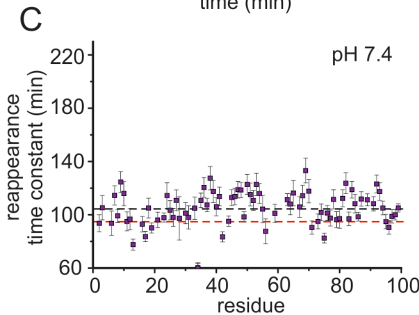
C
pH 7.4
reappearance
time constant (min)
residue

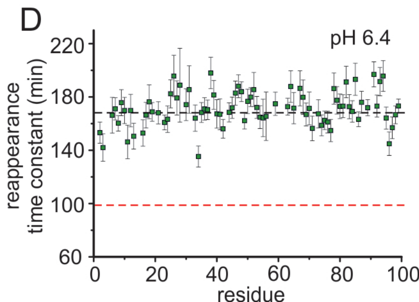
D
pH 6.4
reappearance
time constant (min)
residue

A

pH 7.4

pH 6.4

Amplitude

0.20
0.10
0.00

2.0 nm
15 min

1.7 nm
18 nm
35 min

1.9 nm
55 min

1.9 nm
22 nm
65 min

2.4 nm
85 min

1.7 nm
19 nm
95 min

1.7 nm
105 min

1.7 nm
31 nm
135 min

0.12
0.08
0.04
0.00

1
10
100

Rh (nm)

B

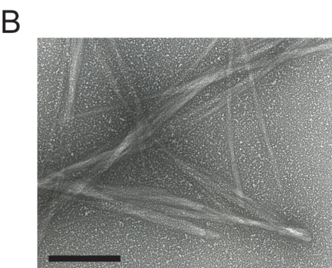

C

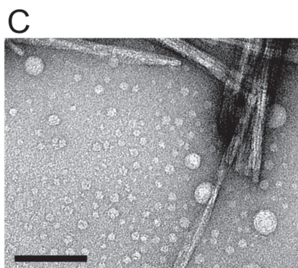

D

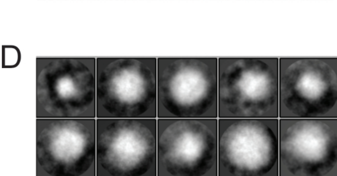

E

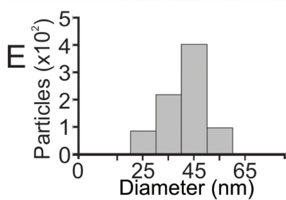

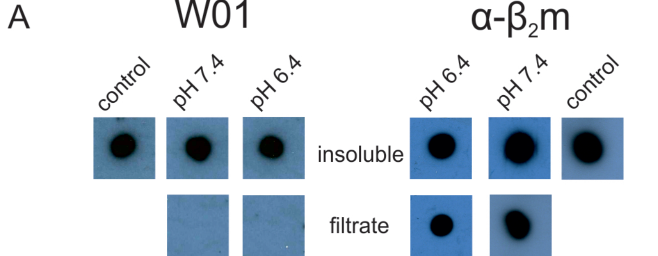
A
W01
α-β2m
control
pH 7.4
pH 6.4
pH 6.4
pH 7.4
control
insoluble
filtrate

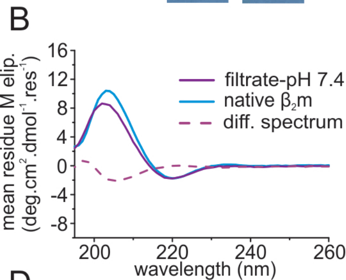
B
mean residue M elip.
(deg.cm2.dmol-1.res-1)
filtrate-pH 7.4
native β2m
diff. spectrum
wavelength (nm)

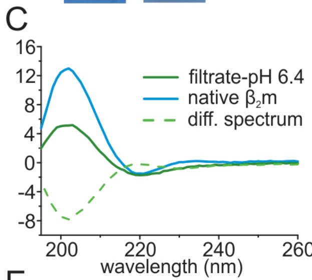
C
filtrate-pH 6.4
native β2m
diff. spectrum
wavelength (nm)

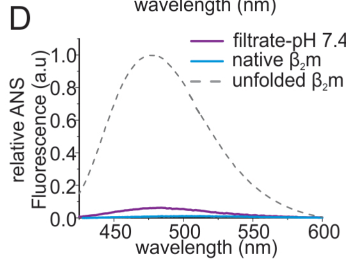
D
relative ANS
Fluorescence (a.u)
filtrate-pH 7.4
native β2m
unfolded β2m
wavelength (nm)

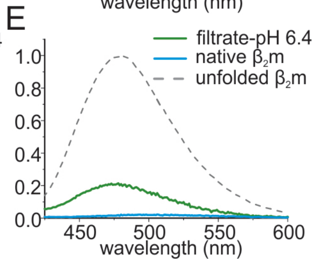
E
filtrate-pH 6.4
native β2m
unfolded β2m
wavelength (nm)

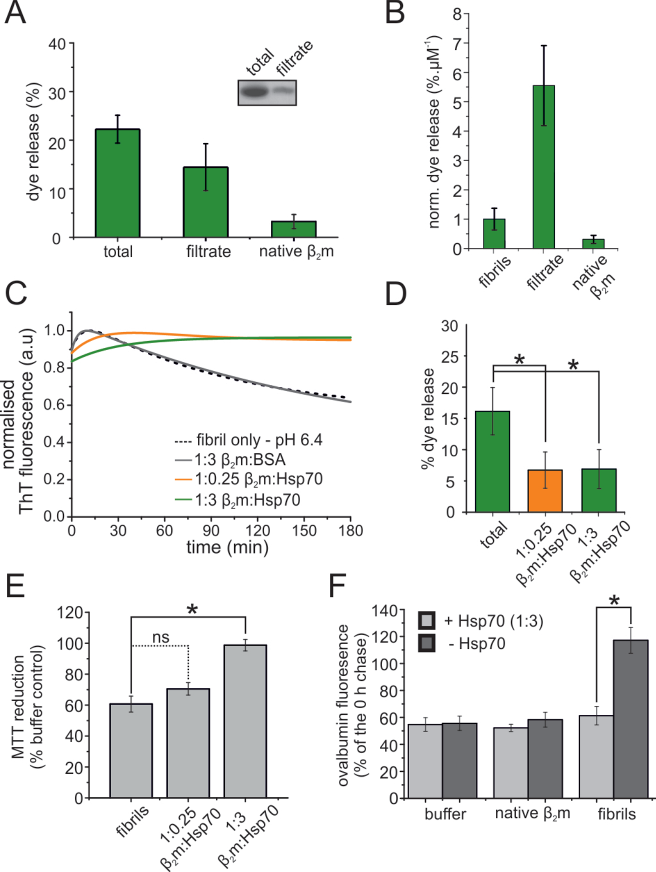
A
40
30
20
10
0
dye release (%)
total
filtrate
total
filtrate
native β2m
B
8
7
6
5
4
3
2
1
0
norm. dye release (%.μM-1)
fibrils
filtrate
native β2m
C
1.0
0.8
0.6
0.4
0.2
0.0
normalised ThT fluorescence (a.u)
0
30
60
90
120
150
180
time (min)
fibril only - pH 6.4
1:3 β2m:BSA
1:0.25 β2m:Hsp70
1:3 β2m:Hsp70
D
30
25
20
15
10
5
0
% dye release
*
*
total
1:0.25 β2m:Hsp70
1:3 β2m:Hsp70
E
120
100
80
60
40
20
0
MTT reduction (% buffer control)
*
ns
fibrils
1:0.25 β2m:Hsp70
1:3 β2m:Hsp70
F
140
120
100
80
60
40
20
0
ovalbumin fluoresence (% of the 0 h chase)
+ Hsp70 (1:3)
- Hsp70
*
buffer
native β2m
fibrils